Elevation of Proenkephalin 143-183 in Cerebrospinal Fluid in Moyamoya Disease

Short title: Elevated PENK 143-183 in Moyamoya Disease

Kinya Yokoyama MD[1,a ¶ #], Mikio Maruwaka MD PhD[1,b ¶], Kazuhiro Yoshikawa PhD[2,c], Yoshio Araki MD PhD[1], Sho Okamoto MD PhD[1], Masaki Sumitomo MD[1,b], Akino Kawamura MD[1,b], Yusuke Sakamoto MD[1,d], Kenzo Shimizu MD[1,e], Takashi Izumi MD PhD[1], Toshihiko Wakabayashi MD PhD[1]

[1] Department of Neurosurgery, Nagoya University Graduate School of Medicine, 65 Tsurumai-cho Showa-ku Nagoya Aichi 466-8550, Japan

[2] Central Research Laboratory, Aichi Medical University School of Medicine, 1-1 Karimata Iwasaku Nagakute Aichi 480-1195, Japan

[a] Present Address: Department of Neurosurgery, Nagoya Medical Center, 4-1-1 San-no-maru Naka-ku Nagoya Aichi 460-0001, Japan

[b] Present Address: Department of Neurosurgery, Toyota Kosei Hospital, 500-1 Ibohara Josui-cho Toyota Aichi 470-0396, Japan

[c] Present Address: Division of Research Creation and Division of Biobank, Research creation support center, Aichi Medical University School of Medicine, 1-1 Karimata Iwasaku Nagakute Aichi 480-1195, Japan

[d]Present Address: Department of Neurosurgery, Ichinomiya Municipal Hospital, 2-2-22 Bunkyo Ichinomiya Aichi 491-8558, Japan

[e] Present Address: Aichi Spine Institute, 41 Gohigasi, Takao, Fuso-cho Niwa-gun, Aichi, 480-0102, Japan

[#]Corresponding author

Kinya Yokoyama

Department of Neurosurgery, Nagoya University Graduate School of Medicine

65 Tsurumai-cho, Showa-ku, Nagoya, Aichi 466-8550, Japan

TEL +81-52-744-2353

FAX +81-52-744-2360

E-mail: swallow_tale@hotmail.com

¶ These authors contributed equally to this work

Abstract

Background: In moyamoya disease (MMD), the causes of differences in clinical features between children and adults and of the dramatic temporal changes in moyamoya vessels are poorly understood. We previously discovered elevated levels of *m/z* 4588 and *m/z* 4473 peptides in cerebrospinal fluid (CSF) in MMD patients. This study examined the amino acid sequences of these peptides and quantified in specimens.

Methods: The *m/z* 4588 and *m/z* 4473 peptides in CSF from MMD patients were purified and concentrated by high-performance liquid chromatography and ultrafiltration. Liquid chromatography coupled with tandem mass spectrometry analysis was performed to identify the amino acid sequences of these peptides. We quantified these peptides in samples using sandwich enzyme-linked immunosorbent assay, and concentrations in CSF were compared between MMD (n=40, 19males; median age, 37years) and non-MMD intracranial disease (n=40, 19males; median age, 39years) as controls.

Results: These peptides were identified as proenkephalin 143-183 (PENK 143-183). The concentration of PENK 143-183 was significantly higher in MMD patients (median, 8,270 pmol/L) than controls (median, 3,760 pmol/L; $P<0.001$) and decreased in an age-dependent manner in MMD ($r=-0.57$; $P<0.001$). The area under the receiver operating characteristic curve in children (age, <18 years) was 0.885 (95% confidence interval, 0.741-1). The correlation between proenkephalin concentration and temporal changes in moyamoya vessels was suggested.

Conclusions: Proenkephalin 143-183 in CSF may offer a helpful diagnostic biomarker in pediatric MMD. The effect of enkephalin peptides through opioid growth factor receptor or delta opioid receptor might be associated with the pathophysiology of MMD.

Key words: Moyamoya disease, angiogenesis, peptide, cerebrospinal fluid, proenkephalin

INTRODUCTION

Moyamoya disease (MMD) is a disorder in which angiogenesis occurs at the base of the cranium, together with progressive stenosis and occlusion in the terminal portion of the internal carotid artery [1,2]. These newly formed vessels are called moyamoya vessels and present with temporal changes on angiography. These vessels tend to increase in the early stages, then regress as the disease progresses [1]. Onset often occurs in children in their teens and adults in their thirties, and the pattern of onset differs with age, often involving brain ischemia in children and intracerebral hemorrhage in adults [3]. Diagnosis is based on characteristic imaging findings and exclusion of other potential diagnoses [2]. No biomarkers useful for diagnosis have been identified to date, but an MMD susceptibility gene has been reported in recent years [4,5]. A relationship between genetic variants and prognosis has been reported [6], but no animal model has yet been developed [7], so the etiology of the disease remains unknown.

MMD is treated by extra-intracranial artery bypass surgery together with indirect revascularization [2,8,9]. This approach takes advantage of the phenomenon that when tissue with blood flow is placed at the brain surface, angiogenesis and anastomosis occur between the tissue and brain surface arteries after surgery. Angiogenesis following indirect revascularization is known to develop more fully in pediatric MMD than in adult MMD [10,11]. As with the etiology of MMD, the causes of these differences in clinical features between children and adults, and of the dramatic temporal changes in moyamoya vessels and intracranial arteries, remain poorly understood.

A number of studies have attempted to elucidate the etiology and pathophysiology of MMD using patient specimens. Specifically, levels of angiogenesis-related cytokines such as basic fibroblast growth factor (b-FGF), hepatocyte growth factor, and transforming growth factor are reportedly significantly higher in surgical specimens of cerebrospinal fluid (CSF),

arterial walls, and dura mater [12-16]. Among these cytokines, b-FGF is reportedly associated with postoperative angiogenesis [13], but no significant difference between pediatric and adult MMD has been reported, and the cause of the decrease in postoperative angiogenesis with age is unknown.

We previously collected intracranial CSF as a surgical specimen from MMD patients and patients with other intracranial diseases. From proteomic analyses using surface-enhanced laser desorption/ionization time-of-flight mass spectrometry (SELDI-TOF MS), we discovered elevated levels of various peptides in the CSF of MMD patients, particularly peptides corresponding to *m/z* 4588 and *m/z* 4473, suggesting these peptides as candidate biomarkers for MMD diagnosis [17]. Later reports showed that levels of the *m/z* 4473 peptide are significantly higher in pediatric MMD than in adult MMD, suggesting a possible relationship with postoperative angiogenesis [18].

The present study was conducted with the following aims: first, to determine the amino acid sequences of the *m/z* 4588 and *m/z* 4473 peptides; second, to quantify these peptides in specimens; third, to investigate whether these peptides are effective biomarkers in diagnosing MMD by examining a greater number of samples than previous studies; and finally, to elucidate the role of these peptides in the pathophysiology of MMD.

METHODS

Patients and Controls

Patient characteristics are shown in Table 1. We collected CSF and serum samples from patients with MMD. We also collected CSF samples from patients with various intracranial diseases other than MMD as controls. MMD samples were collected from the cerebral subarachnoid space of the brain surface during revascularization surgery. Samples from

control patients were collected during craniotomy. No samples were obtained from healthy subjects.

The MMD group consisted of 40 patients diagnosed with the disease who underwent surgery on 58 sides, including bilateral MMD (n = 28, 44 sides), unilateral MMD (n = 6, 6 sides), and quasi-MMD (n = 6, 8 sides). The patterns of onset observed were a decrease in cerebral blood flow but no symptoms (n = 5), transient ischemic attack (TIA, n = 18), cerebral infarction (CI, n = 9), intracerebral hemorrhage (ICH, n = 4), and seizure, headache, or other events (Others, n = 4). The group included 13 children (<18 years old) and 27 adults (≥18 years old). All patients were Japanese. Diagnostic criteria were based on those of the Japanese Research Committee on MMD of the Ministry of Health, Welfare and Labor, Japan (RCMJ) [19]. All MMD patients underwent indirect revascularization, encephalo-myo-synangiosis (EMS), and, if possible, bypass surgery. In MMD patients whose onset occurred with stroke, surgery was performed at least 1 month after onset (median, 6 months; range, 1-60 months). Brain magnetic resonance imaging (MRI) and cerebral angiography were performed within 6 months before surgery and from 9 months to 1 year after surgery. In patients considered to be at high risk based on angiography, only brain MRI was performed.

The control group consisted of 40 patients diagnosed with intracranial diseases other than MMD, including brain ischemias such as internal carotid artery or middle cerebral artery occlusion (n = 5), unruptured brain aneurysm (n = 14), arteriovenous malformations (AVM) (n = 2), brain tumor (n = 9), hydrocephalus (n = 4), and other diseases such as facial spasm or arachnoid cyst (n = 6). The control group included 12 children (<18 years old) and 28 adults (≥18 years old). Overall, age and sex distributions of the control group matched those of the MMD group.

Information was obtained from members of each group either by interview or clinical chart review. Study subjects were recruited at the Department of Neurosurgery, Nagoya

University Hospital, Nagoya, Japan, and the Department of Neurosurgery, Aichi Children's Health and Medical Center, Obu, Aichi, Japan. All experiments were performed at the Central Research Laboratory of the School of Medicine at Aichi Medical University, Nagakute, Aichi, Japan. Approval for this study was given by the Institutional Review Board and Ethics Committee of Nagoya University School of Medicine, Nagoya University, Japan (approval number 586; approval date January 30, 2008); by the Aichi Children's Health and Medical Center Institutional Review Board (approval number 201227; approval date August 1, 2012); and by the Institutional Review Board and Ethics Committee of Aichi Medical University School of Medicine, Japan (approval number 531; approval date May 12, 2008). All subjects provided written informed consent. If a subject was considered too young to consent, informed consent was given by the parent or guardian prior to enrollment in the study.

CSF and serum samples

After collection, CSF samples were centrifuged at 3,000 rpm for 10 min at 4°C. The supernatant was collected and stored at −80°C until used. Peripheral blood samples from MMD patients were allowed to stand undisturbed for 30 min at room temperature and then centrifuged at 3,000 rpm for 10 min at 4°C. The resulting serum was collected and stored at −80°C until used.

Liquid chromatography

Chromatographic separation of the *m/z* 4588 and *m/z* 4473 peptides from CSF samples was achieved using an Accela high-performance liquid chromatography (HPLC) system (Thermo Fisher Scientific, San Jose, CA) equipped with a 5 × 50 mm MonoQ GL 5/50 anion-exchange column (GE Healthcare Bioscience, Amersham, UK). A 500-µL aliquot of each CSF sample was mixed with 50 µL of 1% aqueous ammonia and then injected onto the

column. Buffer A was bicarbonate-carbonate with 10 mmol/L NaCl (pH 10), and buffer B was bicarbonate-carbonate buffer with 1 mol/L NaCl (pH 9.5). Separation was achieved by gradient elution at room temperature and a flow rate of 1 mL/min. The detection wavelength was 280 nm. After separation, the presence of the *m/z* 4588 and *m/z* 4473 peptides was confirmed by SELDI-TOF-MS.

SELDI-TOF-MS

As described in our previous report [17], Q10 ProteinChips (Bio-Rad Laboratories, Hercules, CA) were equilibrated with the appropriate binding/washing buffer for activation. Each sample was then applied, and the chip was incubated in a humid chamber, after which the remaining samples were removed and the chip was washed with binding/washing buffer. The arrays were desalted with distilled water, and saturated energy-absorbing molecule solution (sinapinic acid in 50% acetonitrile and 0.5% trifluoroacetic acid) was applied to each spot prior to analysis of the protein profiles using a ProteinChip reader.

Ultrafiltration and trypsin digestion

The *m/z* 4588 and *m/z* 4473 peptides in the HPLC fraction were purified by ultrafiltration. A total of 500 μL of each HPLC fraction was placed into an Amicon ultracentrifugal filter device 10K (Merck Millipore, Darmstadt, Germany) and centrifuged at 15,000 rpm for 30 min at 4°C. The filtrate was discarded and the filter was washed with distilled water, after which 150 μL of 10% aqueous ammonia was added, and the filter was centrifuged at 15,000 rpm for 30 min. The filtrates of 20 samples were collected, dried in a Speed Vac (Thermo Savant, Holbrook, NY), and dissolved in 50 μL of dissolving solution (10 mM guanidine hydrochloride, 50 mM ammonium bicarbonate, pH 8.0). A 5-μL volume of 100 ng/μL trypsin solution (porcine pancreas; Sigma-Aldrich, St. Louis, MO) was added,

and the sample was then incubated for 4 h at 37°C. To stop the reaction, 1 µL of 1% formic acid was added.

Liquid chromatography coupled with tandem mass spectrometry analysis

Liquid chromatography coupled with tandem mass spectrometry (LC-MS/MS) analysis of trypsin-digested peptides was carried out on an Accela HPLC system (Thermo Fisher Scientific) coupled to an LTQ Velos mass spectrometer (Thermo Fisher Scientific) with a dual-pressure ion trap. Xcalibur 2.1 software was used to evaluate the resulting data. In each run, 25 µL of trypsin-digested sample solution was injected. Separation of analytes was achieved using a Hypersil Gold column (50 × 2.1 mm; Thermo Fisher Scientific). The flow rate was set to 200 µL/min, and the temperature was maintained at 27°C. The mobile phase consisted of two buffers: buffer A was 1% formic acid and buffer B was 1% formic acid in acetonitrile. The following gradient was applied: 0-100% B (0-10 min). MS/MS spectra were collected over the *m/z* scan range 180-2000. The capillary temperature was set to 250°C, source heater temperature to 300°C, source voltage to 3.0 kV, sheath gas to 35 arbitrary units (a.u.), auxiliary gas to 10 a.u., and sweep gas to 0 a.u. Peptides were identified using the MS-Tag database search program of Protein Prospector (University of California, San Francisco; http://prospector.ucsf.edu).

Sandwich enzyme-linked immunosorbent assay

To determine the concentration of proenkephalin (PENK) 143-183 in CSF and serum samples, we used a chemiluminescent sandwich enzyme-linked immunosorbent assay (ELISA) method, as described previously [20]. The protocol was modified as described in the Appendix.

Clinical analysis

To assess angiogenesis after EMS in MMD patients, as we previously reported [18], image findings from the source image of time-of-flight magnetic resonance angiography (TOF MRA) obtained 9 months to 1 year after surgery were used, and scores were given on a 4-point scale from 0 to 3 points for each surgical side based on the progression of newly developed arteries between the temporal muscle and brain surface (Fig. 1).

MMD patients were classified using Suzuki's angiographic grade [1] for each surgical side. Findings from cerebral angiography performed within 6 months before surgery were used for classification. For patients not receiving angiography, 3-dimensional MRA findings were used instead. Patients for whom findings were atypical and unclassifiable were excluded.

Statistical analysis

Concentrations of PENK 143-183 were log-transformed for statistical analyses, as the Kolmogorov-Smirnov test revealed a non-normal distribution of the variables. Welch's t-test was used to compare differences between two groups. The Kruskal-Wallis test was used for comparisons between three or more groups. Spearman's correlation coefficient was used for demonstrating correlations. Values of $P < 0.05$ were taken to indicate statistical significance.

The threshold concentration, sensitivity, and specificity of PENK 143-183 in CSF for diagnosing MMD were obtained by analysis of receiver operating characteristic (ROC) curves, and the area under the curve (AUC) was calculated. In the case of patients who underwent bilateral surgery, the PENK 143-183 concentration in CSF collected during the first surgery was used in analyses, unless otherwise specified.

All statistical analyses were performed using EZR (Saitama Medical Center, Jichi Medical University, Saitama, Japan), which is a graphical user interface for R (The R

Foundation for Statistical Computing, Vienna, Austria). More precisely, EZR is a modified version of R commander designed to add statistical functions frequently used in biostatistics [21].

RESULTS

Identification of the *m/z* 4588 and *m/z* 4473 peptides

Purified, trypsin-digested *m/z* 4588 and *m/z* 4473 fragment peptides were cleaved by ion fragmentation in LC-MS/MS, and the resulting mass spectra were searched against the MS-Tag database. A total of four trypsin-digested fragments were produced, all of which were peptides derived from PENK 143-183 (UniProt knowledgebase: P01210 143-183, http://www.uniprot.org) (Fig. 2). The only difference between the *m*/z 4588 and *m/z* 4473 peptides was the presence of an aspartic acid residue (molecular weight 115) on the N-terminus (Fig. 2).

Concentration of PENK 143-183 in CSF

PENK 143-183 concentrations in CSF were measured in the MMD and control groups using sandwich ELISA and a chemiluminescent substrate. The lower limit of detection for measured concentrations was 25 pmol/L. The median and range of the measured values are shown in Table 1.

The concentration was significantly higher in the MMD group than the control group ($P < 0.001$). Even when evaluating children (<18 years old) and adults (≥18 years old) separately, PENK 143-183 concentrations were significantly higher in the MMD group in both age cohorts, although the difference was more pronounced in children ($P < 0.001$) than in adults ($P < 0.01$) (Fig. 3). In the MMD group, a clear correlation was observed between PENK 143-183 concentration and age ($r = -0.57$; $P < 0.001$), whereas the control group

showed no correlation (P = 0.199) (Fig. 4). These results were the same as those obtained in our previous study using SELDI-TOF-MS [18].

The AUC of the ROC curve was 0.782 (95% confidence interval, 0.68-0.883) for all ages, 0.885 (95% confidence interval, 0.724-1) for children, and 0.714 (95% confidence interval, 0.576-0.853) for adults (Fig. 5).

No significant differences in PENK 143-183 concentration were observed by sex in either the MMD group (P = 0.77) or control group (P = 0.40). In comparisons by diagnosis, no significant differences were observed with disease type in the MMD group (P = 0.36). Likewise, in the control group, no significant differences in concentration were observed between the different diseases (P = 0.12). In the MMD group, no significant differences in PENK 143-183 concentration were observed according to pattern of onset (P = 0.50). In patients who underwent bilateral surgery (n = 18), no significant changes were observed in PENK 143-183 concentration between the first and second surgeries (P = 0.95).

Relationship between PENK 143-183 concentrations in serum and CSF

PENK 143-183 concentrations in serum samples collected at the time of surgery for 19 sides in 17 MMD patients were measured using sandwich ELISA with a chemiluminescent substrate. The lower limit of detection was 12.5 pmol/L. No significant correlation was observed between CSF and serum concentrations in these patients (r = 0.149; P = 0.53) (Fig. 6).

Correlation between angiogenesis after EMS and CSF PENK 143-183

Angiogenesis after EMS was scored for 58 sides in 40 MMD patients. The EMS angiogenesis score was 0 for 12 sides, 1 for 12 sides, 2 for 20 sides, and 3 for 14 sides. A clear negative correlation was observed between the EMS angiogenesis score and age (r =

−0.43; $P < 0.001$), but the correlation between the EMS angiogenesis score and PENK 143-183 in CSF appeared weak ($r = 0.261$; $P = 0.0475$) (Fig. 7).

PENK 143-183 concentration in CSF at each MMD stage

Stage classification was performed for 46 sides (32 MMD patients) that were classifiable from preoperative cerebral angiography findings and for 8 sides (5 patients) that were classified by MRA. Suzuki's angiographic grade was stage 1 for 2 sides, stage 2 for 8 sides, stage 3 for 31 sides, stage 4 for 11 sides, stage 5 for 2 sides, and stage 6 for 0 sides. The distribution of PENK 143-183 concentrations for each grade are shown in Figure 8. The small number of samples for stages 1, 5, and 6 made the data unsuitable for statistical analysis, but the PENK 143-183 concentration rose in stage 2, after which a decreasing trend was seen with stage progression.

DISCUSSION

PENK143-183 as a novel diagnostic biomarker of MMD

This study demonstrated that the *m/z* 4588 and *m/z* 4473 peptides in CSF we previously identified as strong candidate biomarkers for diagnosing MMD are both constituents of PENK 143-183. We also determined concentrations of PENK 143-183 in the CSF of MMD and non-MMD patients by immunoassay and demonstrated a significant elevation in PENK 143-183 concentration in the CSF of MMD patients. The ROC curves obtained from the experimental results showed high AUC values, particularly in pediatric MMD, demonstrating that PENK 143-183 in CSF offers an effective biomarker for MMD diagnosis. Serum concentration of PENK 143-183, however, did not reflect the concentration in CSF.

The presence of PENK 143-183 (also known as PENK 119-159 or midregional proenkephalin) in human CSF was previously confirmed [22], and Ernst et al. recently

reported a method to quantify levels in CSF and serum by sandwich ELISA [20]. With regard to changes in CSF concentrations of PENK 143-183 in intracranial diseases, some reports have described decreases in spinal CSF among patients with acute neuroinflammation or dementia (Alzheimer's disease, dementia with Lewy bodies, frontotemporal dementia, vascular dementia) compared with normal healthy controls [23], but no descriptions of increases have been reported. Our study on MMD is the first to show an increase in PENK 143-183 concentration. MMD is still diagnosed based on imaging findings and exclusion of underlying diseases that can cause similar changes in intracranial arteries [2], and no specific biomarkers exist. However, in actual clinical settings, angiography in MMD patients occasionally presents atypical findings that make diagnosis difficult [24-26]. In 2011, the *RNF 213* p.R4810K polymorphism was reportedly linked with MMD susceptibility [4,5]. Ninety percent of Japanese MMD patients have this gene polymorphism, which has a high diagnostic value [5]. In the present study, a comparison of the MMD and control group patients under 18 years old showed high accuracy when the concentration threshold of PENK 143-183 in CSF was taken to be 9.17 nmol/L, with 92.3% sensitivity and 83.3% specificity (AUC, 0.885; 95% confidence interval, 0.724-1). We therefore believe that PENK 143-183 in CSF potentially offers a novel diagnostic biomarker for MMD, particularly in children.

The concentration of PENK 143-183 in serum did not reflect the concentration in CSF. A previous report by other researchers found that the PENK 143-183 concentration is 100 times greater in CSF than in serum, indicating that PENK 143-183 in CSF is derived from intracranial tissue [20]. In our study, the concentration in CSF was about 80 times greater than that in serum, showing general agreement with previous results (Fig. 6). Recent clinical trials have reported that PENK 143-183 in serum reflects the extent of blood-brain barrier impairment and correlates with the severity and prognosis of cerebral infarction and subarachnoid hemorrhage [27,28]. Sample collection in the present study was performed in

the chronic stage at least 1 month after onset in stroke patients, and so no impairment of the blood-brain barrier was considered to be involved. No previous reports have indicated a correlation between the PENK 143-183 concentration in CSF and peripheral blood, so the present results are novel findings.

Elevation of PENK143-183 CSF concentration and MMD pathophysiology

In our previous study, we found that the concentration of the *m/z* 4473 peptide decreases in an age-dependent manner, suggesting a relationship with angiogenesis after indirect revascularization. In this study, as with the previous study, a clear correlation was observed between the PENK 143-183 concentration in CSF and age and between the EMS angiogenesis score and age in MMD. A slight correlation with angiogenesis after indirect revascularization was also observed (although the possibility remains that age represents a confounding factor). Looking at MMD in each stage in this study, the PENK 143-183 concentration in CSF increased in stage 2, in which moyamoya vessels appear, and then appeared to decrease with stage progression.

PENK 143-183 is a fragmentary peptide produced during the processing of the precursor, proenkephalin A (UniProt knowledgebase: P01210). Human proenkephalin A is widely distributed throughout the body, including the entire nervous system [29-31], adrenal medulla [32], and other body tissues [33-36]. When proenkephalin A is processed, four copies of methionine-enkephalin (Met-ENK) and one copy of leucine-enkephalin (Leu-ENK) are produced [37,38] (Fig. 9). Met-ENK and Leu-ENK are rapidly metabolized and broken down in the CSF and serum, making accurate measurement of concentrations difficult [39,40], but PENK 143-183 is stable in both CSF and serum and thus reflects concentrations of these enkephalin peptides [20].

We developed two hypotheses to explain the elevated PENK 143-183 concentrations seen in the CSF of MMD patients in this study. First, among enkephalin peptides, Met-ENK (also known as opioid growth factor [OGF]) inhibits DNA synthesis via the OGF receptor (OGFr), thereby inhibiting cell proliferation [41-43]. OGF is a potent inhibitor of both normal and tumor cells, and both the peptide and receptor have been detected by antibody staining of tissues in which growth effects have been documented [44]. The inhibitory action of OGF has been observed in the heart, vascular system, corneal epithelium, brain astrocytes, and endothelial cells, as well as mesenchymal and other normal cells [43,45,46]. In an in vitro experiment using chick chorioallantoic membrane, OGF was reported to inhibit angiogenesis [47]. Given these data, PENK 143-183 in MMD CSF was hypothesized to reflect activation of the angiogenesis inhibitory system in MMD. That only a slight correlation was observed between angiogenesis and PENK 143-183 concentration after EMS may have been because PENK 143-183 only indirectly reflects angiogenesis. This hypothesis may to a certain extent explain the phenomenon in which PENK 143-183 increased in stage 2 of Suzuki's angiographic grade, when moyamoya vessels begin to form, and then appeared to decrease thereafter with the regression of moyamoya vessels. However, it remains unclear why the PENK 143-183 concentration decreases in stage 3, when moyamoya vessels are increasing, and whether the stage progresses because of the rise in OGF or moyamoya vessels regress for some other reason and OGF production decreases because cells are no longer actively proliferating.

The second hypothesis is that Met-ENK and Leu-ENK are delta opioid peptides, which act primarily at delta-opioid receptors (DORs). Both compounds are involved in neurotransmission and pain control [48], but studies to date have shown that the opioid system is also related to neuroprotective effects against hypoxia and ischemic events and that these effects are primarily mediated via delta-opioid peptides and DORs [49-52]. DOR

activation decreases the flow of K^+ out of neurons following ischemia [53-56], thereby decreasing neuronal death [57,58]. DOR activation has also been shown to prevent neuronal death by blocking p38 phosphorylation via stimulation of protein kinase C and mitogen-activated protein kinase-ERK1/2 [59-63]. The above evidence indicates that elevated concentrations of PENK 143-183 in MMD CSF may reflect the neuroprotective effects of delta opioids and DORs against brain ischemia. The decrease in PENK 143-183 concentration in CSF in encephalitis and dementia patients compared with healthy controls is attributed to a decrease in proenkephalin-producing cells accompanying brain atrophy [23], but the decrease in PENK 143-183 concentration after increasing with MMD stage and the correlation with age suggest the brain atrophy that occurs with the progression of brain ischemia and aging as a possible cause. Alternatively, in MMD patients, ischemic tolerance due to the delta opioid-DOR system may be more developed than in patients with other cerebral ischemic diseases. The control group in this study included five patients with cerebral ischemic disease, but no clear elevation of PENK 143-183 was seen in comparison with other non-MMD diseases. However, these five patients with brain ischemia were older than the MMD patients, and ischemic tolerance due to the delta opioid-DOR system may decline as a result of aging, regardless of the disease.

Study limitations and future prospects

The major limitation of this study was that healthy normal controls were not examined. However, this was also true in previous studies of MMD using CSF samples [13,15,64,65]. In addition, although patients with other intracranial diseases were included in the control group, no significant differences were observed among them with respect to PENK 143-183 concentration. We were able to match patients for age and sex, and the number of samples for both MMD and control groups was higher than in similar previous studies. In our study,

PENK 143-183 concentrations in intracranial CSF were higher in the MMD group and lower in the control group than in a previous report that measured the concentration in spinal CSF from normal healthy donors [23]. However, protein concentrations are lower in intracranial CSF than spinal CSF. Thus, PENK 143-183 concentration in CSF may also differs from that in lumbar puncture and intracranial samples. Intracranial CSF sampling was selected in this study, because intracranial CSF is in direct contact with the area affected in MMD and because samples could be collected intraoperatively without additional invasiveness. In the future, this problem could be overcome by performing lumbar puncture after induction of anesthesia in MMD patients and comparing the results with intracranial CSF and healthy individuals.

Moreover, important concern is that an increase in PENK 143-183 in MMD merely represents a response to cerebral ischemia. The decrease in PENK 143-183 concentration with age in MMD might reflect decreases in ischemic tolerance with age. In this study, we regarded brain tumors as one of the controls, but tumors also cause ischemia and angiogenesis, and maxim PENK 143-183 concentration in controls was seen in case of pediatric brain tumor. This issue may be asressed by comparisons with specimens from ischemic stroke patients, especially in young individuals.

Furthermore, since the sampling method is invasive and the specimen can be obtained only during surgery under general anesthesia and since 2 days is required for assay result, this method is not useful for determining the surgical procedure (whether to perform EMS, for example), Utility of PENK 143-183 as a diagnostic biomarker may be limited to cases in which diagnosis is difficult based only on angiographic findings and *RNF 213* p.R4810K polymorphism.

Finally, we proposed two hypotheses to explain the elevation in PENK 143-183 concentration in MMD CSF. To test these hypotheses, analysis of the expression of OGFr and

DORs in the blood vessels of stenotic regions may be useful, along with examination of moyamoya vessels and brain tissue in MMD patients. However, the number of autopsies of MMD patients has declined in recent years, and the resulting difficulty in obtaining specimens of affected areas makes this approach problematic [66]. Quantitative analysis of expression levels of DOR and OGFr in the brain using positron emission tomography or single photon emission computed tomography may be effective [67,68].

CONCLUSIONS

Although further research is needed, PENK 143-183 in intracranial CSF probably offers a helpful diagnostic biomarker, especially for pediatric MMD patients. The etiology of MMD remains unclear, but we have shown that enkephalin peptides might be associated with the pathophysiology of MMD.

FUNDING

This work was supported by grants from the Japan Society for the Promotion of Science (Wakate Kenkyu B: 24791496 and 15k19961, https://www.jsps.go.jp). The funders played no role in the study design, data collection and analysis, decision to publish, or preparation of the manuscript.

ACKNOWLEDGMENTS

We are grateful to Minoru Fukayama for performing SELDI-TOF-MS and LC-MS/MS analyses and for his technical support. We are also grateful to Mihoko Kato and Hirokatsu Osawa for collecting CSF samples from pediatric patients.

REFERENCES

1. Suzuki J, Takaku A. Cerebrovascular "moyamoya" disease. Disease showing abnormal net-like vessels in base of brain. *Arch Neurol*. 1969;20:288-299.

2. Research Committee on the Pathology and Treatment of Spontaneous Occlusion of the Circle of Willis; Health Labour Sciences Research Grant for Research on Measures for Infractable Diseases. Guidelines for diagnosis and treatment of moyamoya disease (spontaneous occlusion of the circle of Willis). *Neurol Med Chir (Tokyo)*. 2012;52:245-266.

3. Hoshino H, Izawa Y, Suzuki N, Research Committee on Moyamoya D. Epidemiological features of moyamoya disease in Japan. *Neurol Med Chir (Tokyo)*. 2012;52: 295-298.

4. Kamada F, Aoki Y, Narisawa A, Abe Y, Komatsuzaki S, Kikuchi A. A genome-wide association study identifies RNF213 as the first Moyamoya disease gene. *J Hum Genet*. 2011;56:34-40.

5. Liu W, Morito D, Takashima S, Mineharu Y, Kobayashi H, Hitomi T. Identification of RNF213 as a susceptibility gene for moyamoya disease and its possible role in vascular development. *PLoS One*. 2011;6:e22542.

6. Miyatake S, Miyake N, Touho H, Nishimura-Tadaki A, Kondo Y, Okada I. Homozygous c.14576G>A variant of RNF213 predicts early-onset and severe form of moyamoya disease. *Neurology*. 2012;78:803-810.

7. Sonobe S, Fujimura M, Niizuma K, Nishijima Y, Ito A, Shimizu H. Temporal profile of the vascular anatomy evaluated by 9.4-T magnetic resonance angiography and histopathological analysis in mice lacking RNF213: a susceptibility gene for moyamoya disease. *Brain Res*. 2014;1552:64-71.

8. Karasawa J, Kikuchi H, Furuse S, Sakaki T, Yoshida Y. A surgical treatment of "moyamoya" disease "encephalo-myo synangiosis". *Neurol Med Chir (Tokyo)*. 1977;17:29-

37.

9. Kinugasa K, Mandai S, Kamata I, Sugiu K, Ohmoto T. Surgical treatment of moyamoya disease: operative technique for encephalo-duro-arterio-myo-synangiosis, its follow-up, clinical results, and angiograms. *Neurosurgery*. 1993;32:527-531.

10. Houkin K, Kamiyama H, Abe H, Takahashi A, Kuroda S. Surgical therapy for adult moyamoya disease. Can surgical revascularization prevent the recurrence of intracerebral hemorrhage? *Stroke*. 1996;27:1342-1346.

11. Czabanka M, Vajkoczy P, Schmiedek P, Horn P. Age-dependent revascularization patterns in the treatment of moyamoya disease in a European patient population. *Neurosurg Focus*. 2009;26:E9.

12. Takahashi A, Sawamura Y, Houkin K, Kamiyama H, Abe H. The cerebrospinal fluid in patients with moyamoya disease (spontaneous occlusion of the circle of Willis) contains high level of basic fibroblast growth factor. *Neurosci Lett*. 1993;160:214-216.

13. Yoshimoto T, Houkin K, Takahashi A, Abe H. Angiogenic factors in moyamoya disease. *Stroke*. 1996;27:2160-2165.

14. Houkin K, Yoshimoto T, Abe H, Nagashima K, Nagashima M, Takeda M. Role of basic fibroblast growth factor in the pathogenesis of moyamoya disease. *Neurosurg Focus*. 1998;5:e2.

15. Nanba R, Kuroda S, Ishikawa T, Houkin K, Iwasaki Y. Increased expression of hepatocyte growth factor in cerebrospinal fluid and intracranial artery in moyamoya disease. *Stroke*. 2004;35:2837-2842.

16. Hojo M, Hoshimaru M, Miyamoto S, Taki W, Nagata I, Asahi M. Role of transforming growth factor-beta1 in the pathogenesis of moyamoya disease. *J Neurosurg*. 1998;89:623-629.

17. Araki Y, Yoshikawa K, Okamoto S, Sumitomo M, Maruwaka M, Wakabayashi T.

Identification of novel biomarker candidates by proteomic analysis of cerebrospinal fluid from patients with moyamoya disease using SELDI-TOF-MS. *BMC Neurol*. 2010;10:112.

18. Maruwaka M, Yoshikawa K, Okamoto S, Araki Y, Sumitomo M, Kawamura A. Biomarker research for moyamoya disease in cerebrospinal fluid using surface-enhanced laser desorption/ionization time-of-flight mass spectrometry. *J Stroke Cerebrovasc Dis*. 2015;24:104-111.

19. Fukui M. Guidelines for the diagnosis and treatment of spontaneous occlusion of the circle of Willis ('moyamoya' disease). Research Committee on Spontaneous Occlusion of the Circle of Willis (Moyamoya Disease) of the Ministry of Health and Welfare, Japan. *Clin Neurol Neurosurg*. 1997;99 Suppl 2:S238-S240.

20. Ernst A, Kohrle J, Bergmann A. Proenkephalin A 119-159, a stable proenkephalin A precursor fragment identified in human circulation. *Peptides*. 2006;27:1835-1840.

21. Kanda Y. Investigation of the freely available easy-to-use software 'EZR' for medical statistics. *Bone Marrow Transplant*. 2013;48:452-458.

22. Stark M, Danielsson O, Griffiths WJ, Jornvall H, Johansson J. Peptide repertoire of human cerebrospinal fluid: novel proteolytic fragments of neuroendocrine proteins. *J Chromatogr B Biomed Sci Appl*. 2001;754:357-367.

23. Ernst A, Buerger K, Hartmann O, Dodel R, Noelker C, Sommer N. Midregional Proenkephalin A and N-terminal Protachykinin A are decreased in the cerebrospinal fluid of patients with dementia disorders and acute neuroinflammation. *J Neuroimmunol*. 2010;221:62-67.

24. Kataoka H, Miyamoto S, Nagata I, Hatano T, Kano H, Hashimoto N. Moyamoya disease showing atypical angiographic findings--two case reports. *Neurol Med Chir (Tokyo)*. 1999;39:294-298.

25. Chung SJ, Lee HS, Yoo HS, Kim KM, Lee KJ, Kim JS. A case of isolated middle

cerebral artery stenosis with hemichorea and moyamoya pattern collateralization. *J Mov Disord*. 2013;6:13-16.

26. Inamura A, Nomura S, Sadahiro H, Oku T, Ishihara H, Suzuki M. Multiple encephalogaleoperiosteal synangiosis for bilateral carotid artery stenosis in a 13-year-old girl: a case report. Childs Nerv Syst. 2016;32:877-880.

27. Doehner W, von Haehling S, Suhr J, Ebner N, Schuster A, Nagel E. Elevated plasma levels of neuropeptide proenkephalin a predict mortality and functional outcome in ischemic stroke. *J Am Coll Cardiol*. 2012;60:346-354.

28. Chen XL, Yu BJ, Chen MH. Circulating levels of neuropeptide proenkephalin A predict outcome in patients with aneurysmal subarachnoid hemorrhage. *Peptides*. 2014;56:111-115.

29. Hughes J, Smith TW, Kosterlitz HW, Fothergill LA, Morgan BA, Morris HR. Identification of two related pentapeptides from the brain with potent opiate agonist activity. *Nature*. 1975;258:577-580.

30. Pittius CW, Seizinger BR, Mehraein P, Pasi A, Herz A. Proenkephalin-A-derived peptides are present in human brain. *Life Sci*. 1983;33 Suppl 1:41-44.

31. Spruce BA, Curtis R, Wilkin GP, Glover DM. A neuropeptide precursor in cerebellum: proenkephalin exists in subpopulations of both neurons and astrocytes. *EMBO J*. 1990;9:1787-1795.

32. Stern AS, Jones BN, Shively JE, Stein S, Undenfriend S. Two adrenal opioid polypeptides: proposed intermediates in the processing of proenkephalin. *Proc Natl Acad Sci U S A*. 1981;78:1962-1966.

33. Rosen H, Polakiewicz RD, Benzakine S, Bar-Shavit Z. Proenkephalin A in bone-derived cells. *Proc Natl Acad Sci U S A*. 1991;88:3705-3709.

34. Plotnikoff NP, Faith RE, Murgo AJ, Herberman RB, Good RA. Methionine

enkephalin: a new cytokine--human studies. *Clin Immunol Immunopathol*. 1997;82:93-101.

35. Kamphuis S, Eriksson F, Kavelaars A, Zijlstra J, van de Pol M, Kuis W. Role of endogenous pro-enkephalin A-derived peptides in human T cell proliferation and monocyte IL-6 production. *J Neuroimmunol*. 1998;84:53-60.

36. Rosen H, Krichevsky A, Bar-Shavit Z. The enkephalinergic osteoblast. *J Bone Miner Res*. 1998;13:1515-1520.

37. Goumon Y, Strub JM, Moniatte M, Nullans G, Poteur L, Hubert P. The C-terminal bisphosphorylated proenkephalin-A-(209-237)-peptide from adrenal medullary chromaffin granules possesses antibacterial activity. *Eur J Biochem*. 1996;235:516-525.

38. Kojima K, Kilpatrick DL, Stern AS, Jones BN, Udenfriend S. Proenkephalin: a general pathway for enkephalin biosynthesis in animal tissues. *Arch Biochem Biophys*. 1982;215:638-643.

39. Mosnaim AD, Puente J, Wolf ME, Callaghan OH, Busch R, Diamond S. Studies of the in vitro human plasma degradation of methionine-enkephalin. *Gen Pharmacol*. 1988;19:729-733.

40. Mosnaim AD, Puente J, Saavedra R, Diamond S, Wolf ME. In vitro human plasma leucine(5)-enkephalin degradation is inhibited by a select number of drugs with the phenothiazine molecule in their chemical structure. *Pharmacology*. 2003;67:6-13.

41. Cheng F, Zagon IS, Verderame MF, McLaughlin PJ. The opioid growth factor (OGF)-OGF receptor axis uses the p16 pathway to inhibit head and neck cancer. *Cancer Res*. 2007;67:10511-10518.

42. Cheng F, McLaughlin PJ, Verderame MF, Zagon IS. The OGF-OGFr axis utilizes the p21 pathway to restrict progression of human pancreatic cancer. *Mol Cancer*. 2008;7:5.

43. Cheng F, McLaughlin PJ, Verderame MF, Zagon IS. The OGF-OGFr axis utilizes the p16INK4a and p21WAF1/CIP1 pathways to restrict normal cell proliferation. *Mol Biol Cell*.

2009;20:319-327.

44. McLaughlin PJ, Zagon IS. The opioid growth factor-opioid growth factor receptor axis: homeostatic regulator of cell proliferation and its implications for health and disease. *Biochem Pharmacol*. 2012;84:746-755.

45. Zagon IS, Ruth TB, Leure-duPree AE, Sassani JW, McLaughlin PJ. Immunoelectron microscopic localization of the opioid growth factor receptor (OGFr) and OGF in the cornea. *Brain Res*. 2003;967:37-47.

46. Zagon IS, Ruth TB, McLaughlin PJ. Nucleocytoplasmic distribution of opioid growth factor and its receptor in tongue epithelium. *Anat Rec A Discov Mol Cell Evol Biol*. 2005;282:24-37.

47. Blebea J, Mazo JE, Kihara TK, Vu JH, McLaughlin PJ, Atnip RG. Opioid growth factor modulates angiogenesis. *J Vasc Surg*. 2000;32:364-373.

48. Akil H, Watson SJ, Young E, Lewis ME, Khachaturian H, Walker JM. Endogenous opioids: biology and function. *Annu Rev Neurosci*. 1984;7:223-255.

49. Xia Y, Jiang C, Haddad GG. Oxidative and glycolytic pathways in rat (newborn and adult) and turtle brain: role during anoxia. *Am J Physiol*. 1992;262:R595-R603.

50. Sick TJ, Rosenthal M, LaManna JC, Lutz PL. Brain potassium ion homeostasis, anoxia, and metabolic inhibition in turtles and rats. *Am J Physiol*. 1982;243:R281-R288.

51. Xia Y, Haddad GG. Major difference in the expression of delta- and mu-opioid receptors between turtle and rat brain. *J Comp Neurol*. 2001;436:202-210.

52. Zhang J, Haddad GG, Xia Y. Delta-, but not mu- and kappa-, opioid receptor activation protects neocortical neurons from glutamate-induced excitotoxic injury. *Brain Res*. 2000;885:143-153.

53. Chao D, Bazzy-Asaad A, Balboni G, Xia Y. Delta-, but not mu-, opioid receptor stabilizes K(+) homeostasis by reducing Ca(2+) influx in the cortex during acute hypoxia. *J*

Cell Physiol. 2007;212:60-67.

54. Chao D, Donnelly DF, Feng Y, Bazzy-Asaad A, Xia Y. Cortical delta-opioid receptors potentiate K+ homeostasis during anoxia and oxygen-glucose deprivation. *J Cereb Blood Flow Metab*. 2007;27:356-368.

55. Chao D, Bazzy-Asaad A, Balboni G, Salvadori S, Xia Y. Activation of DOR attenuates anoxic K+ derangement via inhibition of Na+ entry in mouse cortex. *Cereb Cortex*. 2008;18:2217-2227.

56. Chao D, Balboni G, Lazarus LH, Salvadori S, Xia Y. Na+ mechanism of delta-opioid receptor induced protection from anoxic K+ leakage in the cortex. *Cell Mol Life Sci*. 2009;66:1105-1115.

57. Liu D, Slevin JR, Lu C, Chan SL, Hansson M, Elmer E. Involvement of mitochondrial K+ release and cellular efflux in ischemic and apoptotic neuronal death. *J Neurochem*. 2003;86:966-979.

58. Wei L, Yu SP, Gottron F, Snider BJ, Zipfel GJ, Choi DW. Potassium channel blockers attenuate hypoxia- and ischemia-induced neuronal death in vitro and in vivo. *Stroke*. 2003;34:1281-1286.

59. Ma MC, Qian H, Ghassemi F, Zhao P, Xia Y. Oxygen-sensitive {delta}-opioid receptor-regulated survival and death signals: novel insights into neuronal preconditioning and protection. *J Biol Chem*. 2005;280:16208-16218.

60. Narita M, Kuzumaki N, Miyatake M, Sato F, Wachi H, Seyama Y. Role of delta-opioid receptor function in neurogenesis and neuroprotection. *J Neurochem*. 2006;97:1494-1505.

61. Feng Y, Chao D, He X, Yang Y, Kang X, L HL. A novel insight into neuroprotection against hypoxic/ischemic stress. *Sheng Li Xue Bao*. 2009;61:585-592.

62. Ke S, Dian-san S, Xiang-rui W. Delta opioid agonist [D-Ala2, D-Leu5] enkephalin

(DADLE) reduced oxygen-glucose deprivation caused neuronal injury through the MAPK pathway. *Brain Res*. 2009;1292:100-106.

63. Peng PH, Huang HS, Lee YJ, Chen YS, Ma MC. Novel role for the delta-opioid receptor in hypoxic preconditioning in rat retinas. J Neurochem. 2009;108: 741-754.

64. Soriano SG, Cowan DB, Proctor MR, Scott RM. Levels of soluble adhesion molecules are elevated in the cerebrospinal fluid of children with moyamoya syndrome. *Neurosurgery*. 2002;50:544-549.

65. Kim SK, Yoo JI, Cho BK, Hong SJ, Kim YK, Moon JA. Elevation of CRABP-I in the cerebrospinal fluid of patients with Moyamoya disease. *Stroke*. 2003;34:2835-2841.

66. Houkin K, Ito M, Sugiyama T, Shichinohe H, Nakayama N, Kazumata K. Review of past research and current concepts on the etiology of moyamoya disease. *Neurol Med Chir (Tokyo)*. 2012;52:267-277.

67 Madar I, Lever JR, Scheffel U, Ravert HT, Musachio JL. Imaging of delta opioid receptors in human brain by N1′ - ([^{11}C]methyl)naltrindole and PET. *Synapse*.1996;24: 19–28.

68 Lever, John R. PET and SPECT imaging of the opioid system: receptors, radioligands and avenues for drug discovery and development. *Current Pharmaceutical Design.* 2007;13:33-49.

Table 1. Patient characteristics.

	No. of patients (sides)	Age, median (range)	Male (female)	Concentration of PENK 143-183 in CSF, median (range) (pmol/L)
MMD				
Total	40 (58)	37 (1-66)	19 (21)	8,270 (1,140-20,100)
Diagnosis				
Bilateral	28 (44)	39 (1-54)	16 (12)	8,270 (2,450-20,100)
Unilateral	6 (6)	29 (9-48)	1 (5)	10,900 (4,390-15,800)
Quasi	6 (8)	33 (2-66)	2 (4)	7,160 (1,140-12,400)
Onset				
Asymptomatic	5	44 (3-49)	3 (2)	6,340 (4,500-13,500)
TIA	18	32 (7-66)	9 (9)	8,870 (2,450-16,800)
CI	9	28 (1-44)	5 (4)	9,800 (1,140-13,500)
ICH	4	42 (9-54)	1 (3)	6,370 (4,090-10,200)
Others	4	23 (6-42)	1 (3)	11,400 (5,550-20,100)
Age				
<18 (Pediatric)	13	7 (1-16)	10 (3)	13,500 (6,470-20,100)
≥18 (Adult)	27	40 (18-66)	9 (18)	6,580 (1,140-16,800)
Controls				
Total	40	39 (0-73)	19 (21)	3,760 (307-18,400)
Diagnosis				
Ischemia	5	69 (56-71)	2 (3)	4,060 (2,550-8,250)
Aneurysm	14	62.5 (27-73)	4 (10)	6,120 (3,190-10,800)

AVM	2	34 (33-35)	1 (1)	5,800 (3,180-8,420)
Tumor	9	20.5 (0-47)	5 (4)	3,070 (307-18,400)
Hydrocephalus	4	3.5 (0-32)	3 (1)	4,050 (1,020-8,760)
Others	6	5.5 (0-54)	4 (2)	2,760 (707-5,460)
Age				
<18 (Pediatric)	12	1 (0-15)	8 (4)	3,030 (806-18,400)
≥18 (Adult)	28	57.5 (26-73)	11 (17)	3,950 (307-10,800)

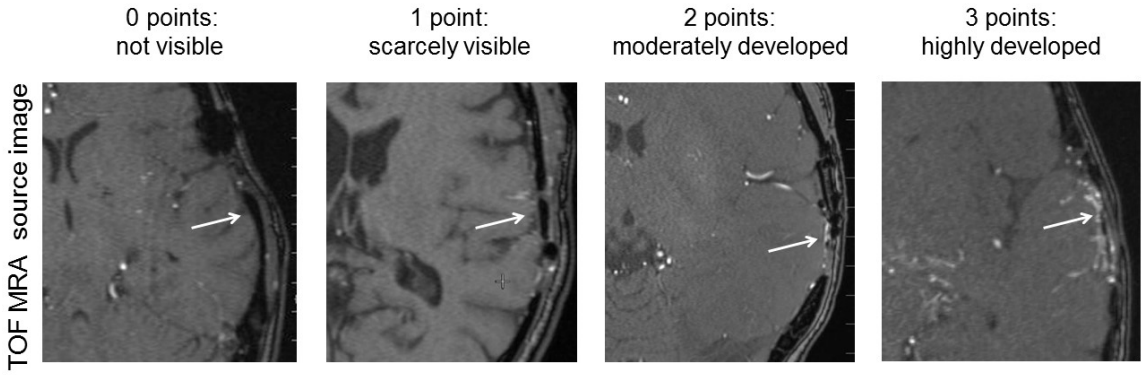

Figure 1. Angiogenesis scores after EMS.

To assess angiogenesis after EMS, the findings of postoperative time-of-flight magnetic resonance angiography (TOF MRA) were used, and scores were given on a 4-point scale

from 0 to 3 points for each surgical side based on the newly developed arteries between the temporal muscle and brain surface (white arrow).

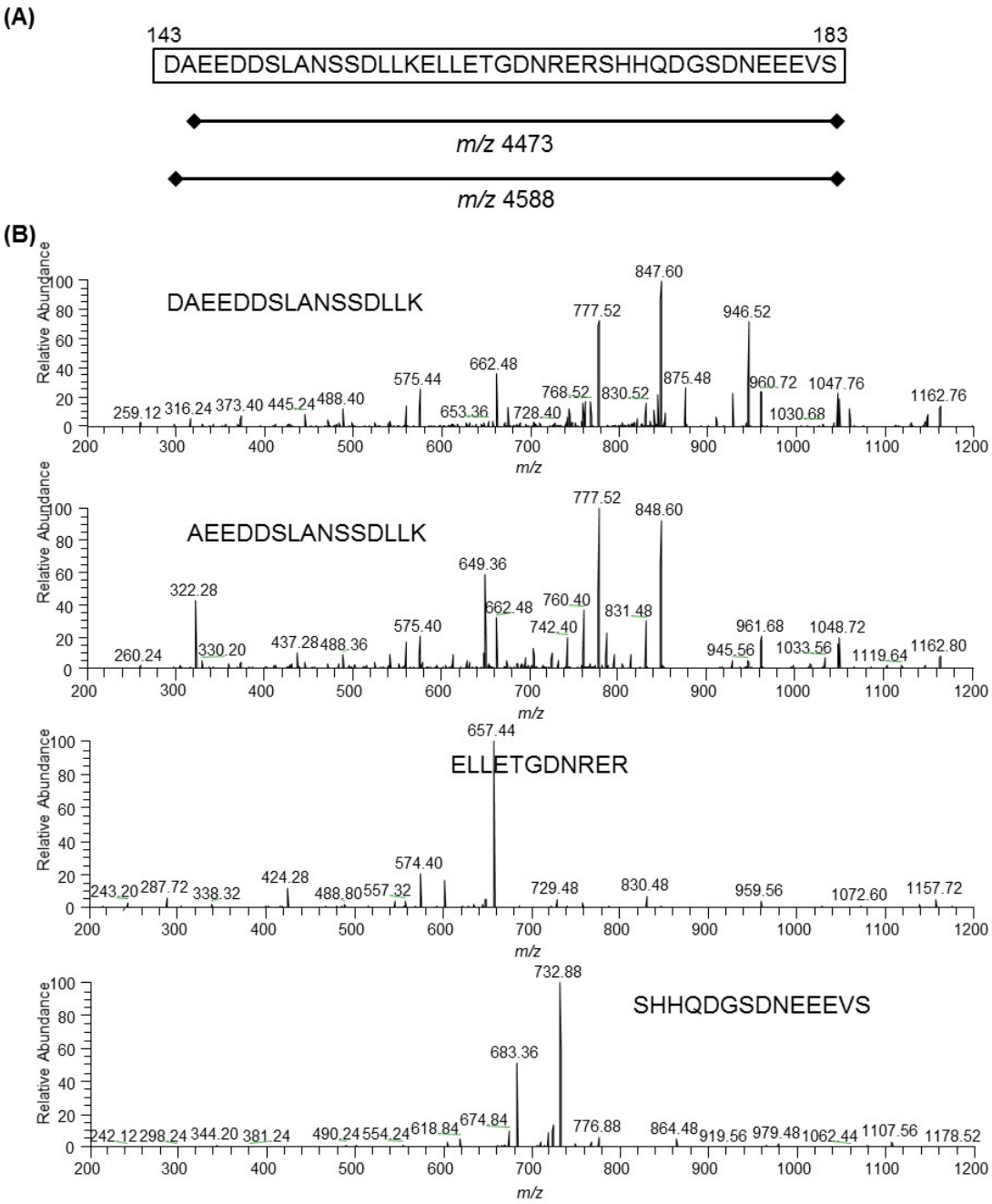

Figure 2. Identification of the *m/z* 4473 and *m/z* 4588 peptides.

(A) Relationship between the proenkephalin (PENK) 143-183 amino acid sequence and the *m/z* 4473 and *m/z* 4588 peptides. The *m/z* 4588 peptide was identified as PENK 143-183, and the only difference with *m/z* 4473 was the presence of an aspartic acid residue (D, molecular weight 115) on the N-terminus. (B) Amino acid sequences corresponding to the MS/MS spectra of the *m/z* 4473 and *m/z* 4588 peptides after trypsin digestion. Four peptide fragments cleaved C-terminally to lysine (K) and arginine (R) are produced, all of which are peptides that constitute PENK 143-183.

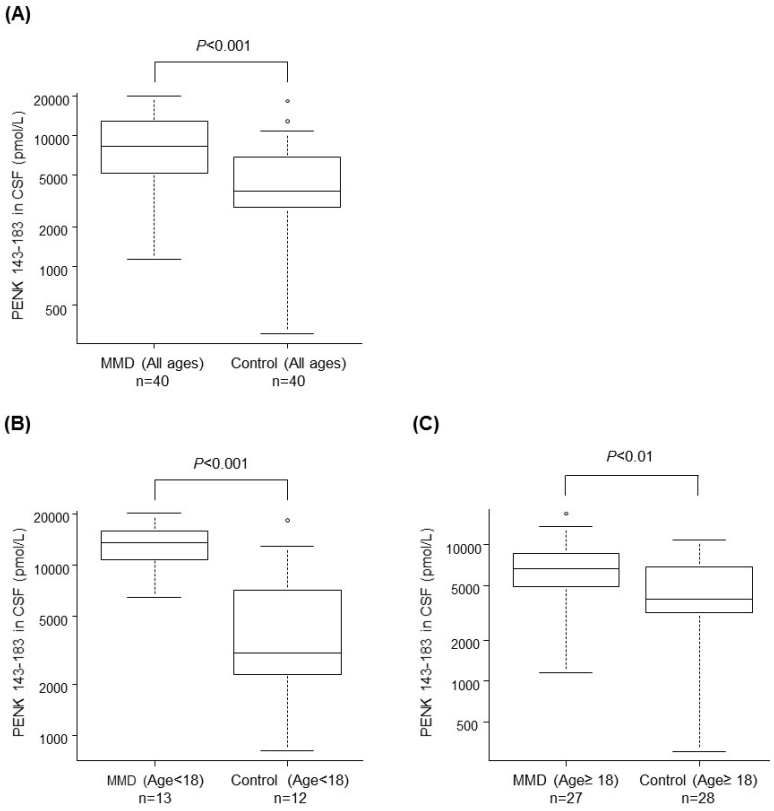

Figure 3. Comparison of the CSF PENK 143-183 concentrations in the MMD and control groups.

(A) Comparison of MMD patients and controls in each age range; $P < 0.001$. (B) Comparison of MMD patients and controls <18 years old; $P < 0.001$. (C) Comparison of MMD patients and controls ≥18 years old; $P < 0.01$. In all comparisons, PENK 143-183 concentrations in

CSF were significantly higher in the MMD group. This difference was particularly marked in children.

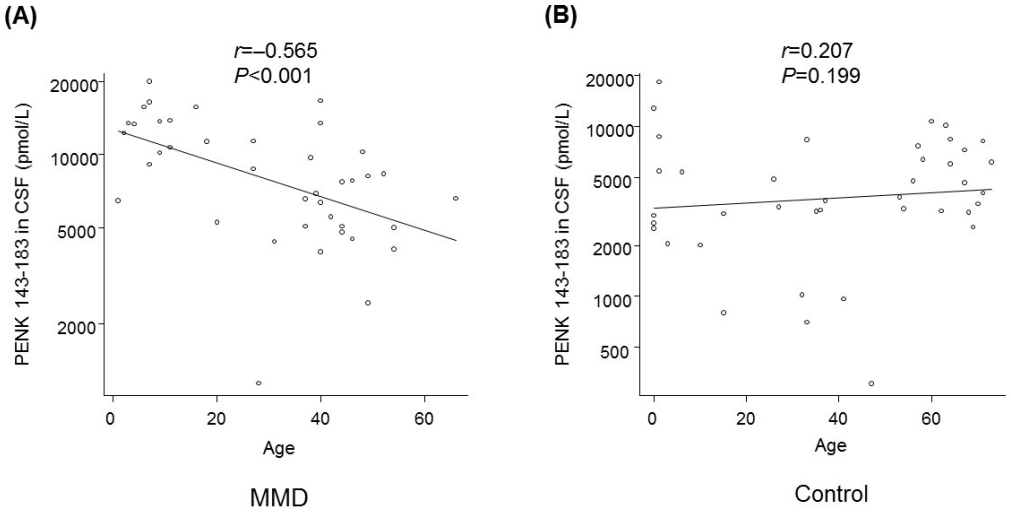

Figure 4. Correlation between PENK 143-183 concentration in CSF and age.

In the MMD group (A), a clear correlation was observed between PENK 143-183 concentration and age ($r = -0.57$; $P < 0.001$), but the control group (B) showed no correlation ($P = 0.199$)

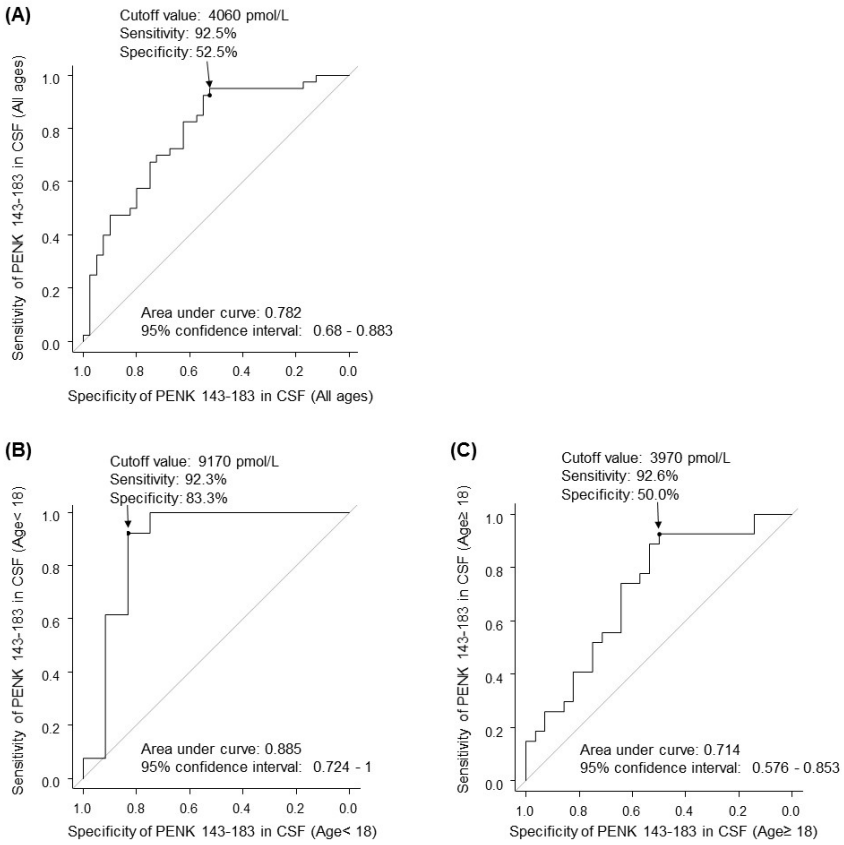

Figure 5. Receiver operating characteristic curve analysis for identifying MMD patients from controls.

(A) All ages. (B) Children (<18 years old). (C) Adults (≥18 years old).

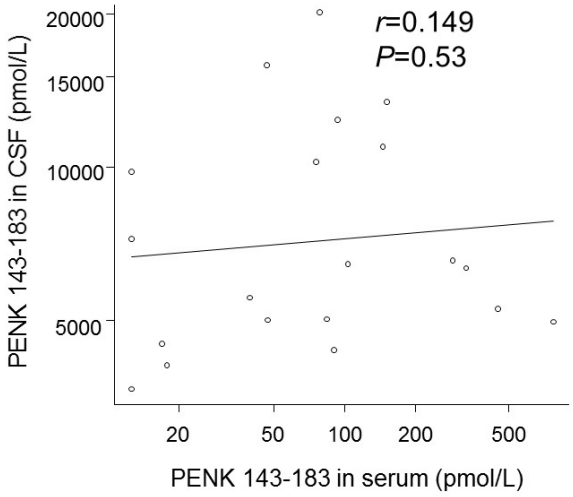

Figure 6. Correlation between PENK 143-183 concentrations in MMD CSF and serum. No significant correlations were observed (r = 0.149; P = 0.53). The concentration in CSF (median, 6410 pmol/L; range, 3680-2010 pmol/L) was about 80 times greater than that in serum (median, 81.4 pmol/L; range, 12.5-773 pmol/L).

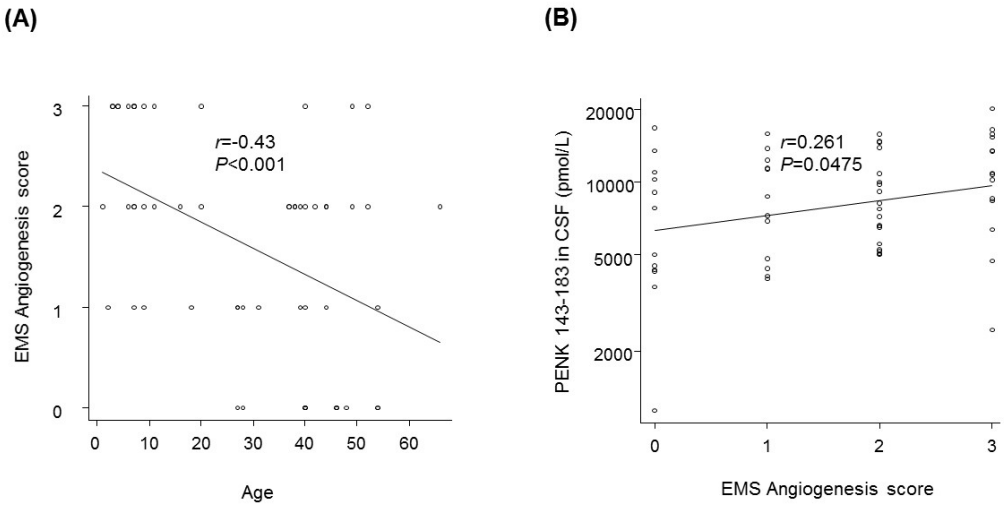

Figure 7. Correlation between postoperative angiogenesis and age or PENK 143-183 concentration in CSF.

(A) A clear correlation was observed between age and angiogenesis score ($r = -0.43$; $P < 0.001$), (B) whereas the correlation between PENK 143-183 concentration in CSF and angiogenesis score was weak ($r = 0.261$; $P = 0.0475$).

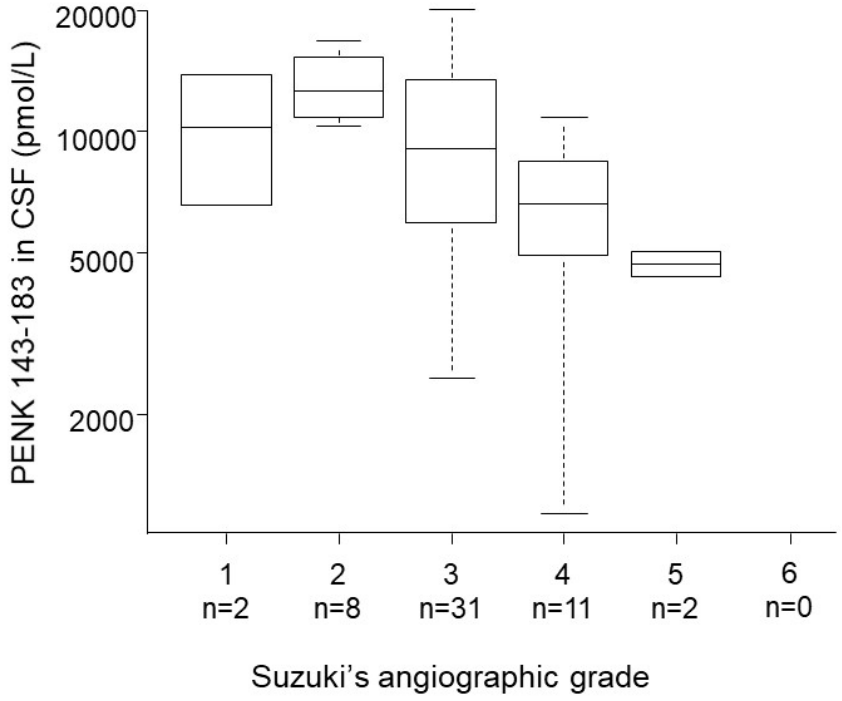

Figure 8. PENK 143-183 concentration in CSF at each stage in the Suzuki's angiographic grade scheme.

The small number of samples for stages 1, 5, and 6 made the data unsuitable for statistical analysis, but the PENK 143-183 concentration in CSF increased in stage 2, after which a decreasing trend with stage progression was observed.

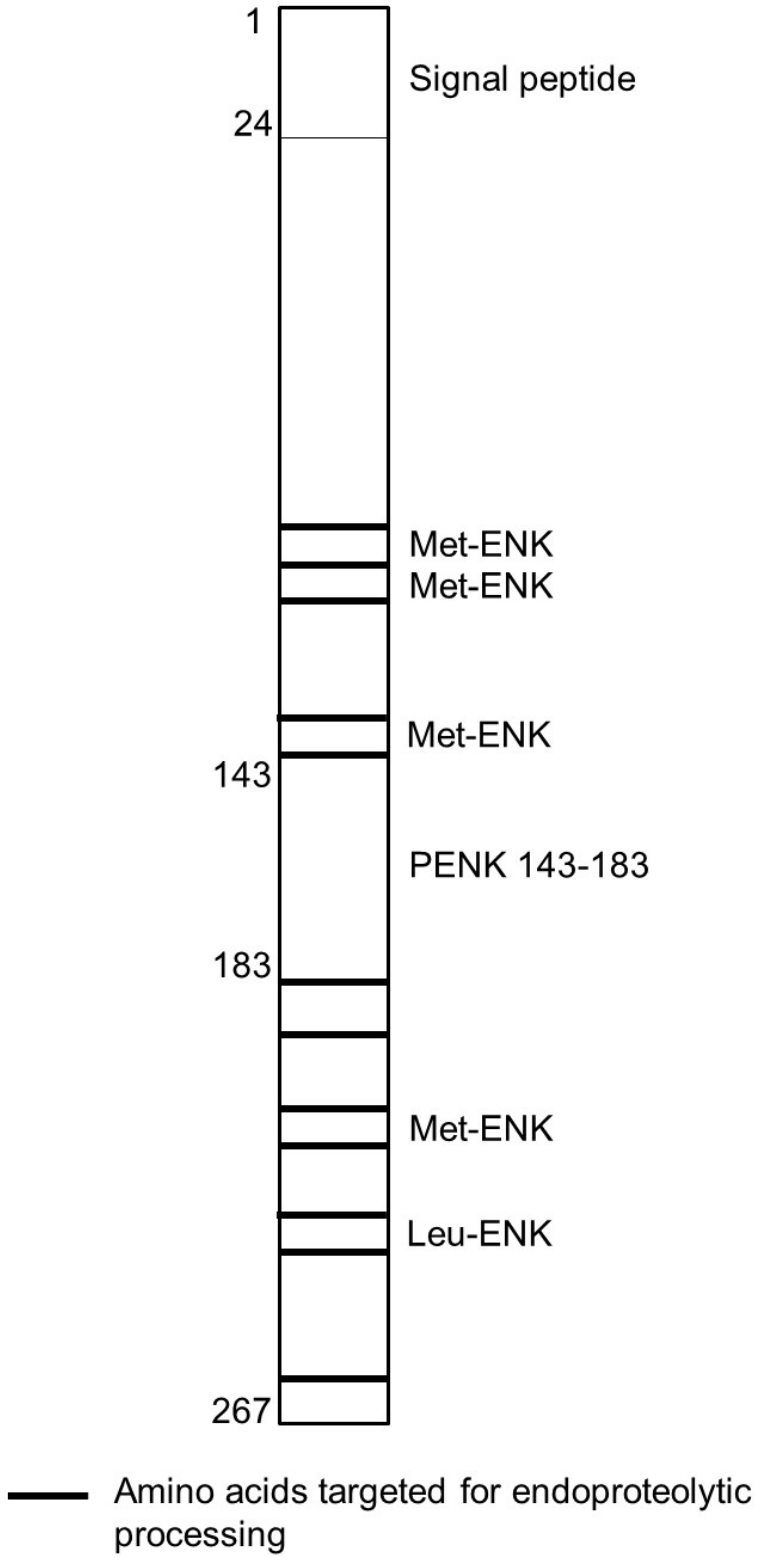

Figure 9. Structure of human proenkephalin A.

During physiological processing, proenkephalin A produce four copies of methionine-enkephalin (Met-ENK), one copy of leucine-enkephalin (Leu-ENK), and one copy of

proenkephalin 143-183.

APPENDIX

Sandwich enzyme-linked immunosorbent assay (details)

Ninety-six-well polystyrene plates (Thermo Fisher Scientific) were coated with 5 µg/mL of anti–PENK 143-160 antibody (Immunogen affinity purified, rabbit polyclonal, BioGate, Gifu, Japan) diluted in 100 µL of phosphate-buffered saline (PBS), pH 7.2, for 2 h at 37°C, and the plates were then washed with PBS. The plates were blocked with 200 µL of 1% skim milk for 2 h at 37°C and then washed with PBS containing 0.05% Tween 20 (PBST). Dilutions of the synthetic peptide PENK 143-183 (BioGate) were used as calibrators. The peptide was diluted in assay buffer (PBST) for CSF samples and in fetal bovine serum (FBS) for serum samples. CSF samples were diluted 1:20 in assay buffer, whereas serum samples were used undiluted. Next, 100 µL of sample/sample dilution or standard peptide solution was added and the plates were incubated for 20 h at 4°C and then washed with PBST. For detection, 5 µg/mL of anti–PENK 168-180 antibody (Immunogen affinity purified, goat polyclonal antibody; Abcam, Tokyo, Japan) diluted in 100 µL of PBS, pH 7.2, containing 0.05% Tween 20 and 1% skim milk was added and incubated for 1 h at room temperature, followed by washing with PBST. The secondary antibody was 0.4 µg/mL of anti–goat immunoglobulin (Ig)G conjugated to horseradish peroxidase (HRP) (mouse antibody; Santa Cruz Biotechnology, Santa Cruz, CA) diluted in 100 µL of PBS, pH 7.2, containing 0.05% Tween 20, 1% skim milk, and 10 µg/mL of purified normal rabbit IgG. The plate was incubated for 1 h at room temperature and then washed with PBS. Finally, 100 µL of HRP substrate solution (BM Chemiluminescence ELISA Substrate; Roche Lifescience, Penzberg, Germany) was added and incubated for 3 min at room temperature, and the absorbance at 450 nm was measured with a reduction at 570 nm using a Spectramax M5 microplate reader (Molecular Devices, Sunnyvale, CA) within 30 min. A

standard curve was established by serial dilution of the calibrator. All samples and calibrators were analyzed in triplicate. Sensitivity was determined by measuring the absorbance in 10 wells of assay buffer for CSF and FBS for serum and adding a value twice that of the standard deviation to the respective means. The corresponding PENK 143-183 concentration was obtained from the calibration curve.